Effects of Hydrogen Bonding to Amines on the Phenol/Phenoxyl Radical Oxidation

Ying Fang, Lei Liu,*,† Yong Feng, Xiao-Song Li,‡ and Qing-Xiang Guo*

Department of Chemistry, University of Science and Technology of China, Hefei 230026, P. R. China

Received: December 5, 2001; In Final Form: February 26, 2002

Theoretical calculations were performed to study the effects of hydrogen bonding to various amines on the oxidation of phenol to phenoxyl radical. It was found that with ammonia as the hydrogen bond acceptor the phenol oxidation process was a barrierless proton-coupled electron transfer and the shift of the adiabatic phenol oxidation potential by ammonia in the gas phase was as large as about 1 eV. For other amines, it was found that depending on the basicity of the amine, the effects of hydrogen bonding to different amines on the phenol oxidation varied. For those amines that had a proton affinity larger than ca. 204 kcal/mol, the oxidation of the phenol−amine complexes caused a proton transfer and the proton-transferred structure was the only minimum found on the potential surface after oxidation. When the proton affinity of the amine was located in the range of ca. 190−197 kcal/mol, both the proton-transferred and nonproton-transferred structures were found to be minima for the oxidized complex. However, when the proton affinity of the amine was smaller than ca. 189 kcal/mol, no proton transfer occurred in the oxidation. The shift of the adiabatic oxidation potential was found to be roughly in linear correlation with the proton affinity of the amine. For substituted aminoacetylenes, the shift of the adiabatic oxidation potential was also found to be in linear correlation with the Hammett σ_p substituent constants. Finally, it was found that the phenol−imidazole−formate complex was not a good model for the tyrosine oxidation in photosystem II, because this complex had a too low oxidation potential. In fact, because of the strong electron donating effects of formate, in addition to phenol the imidazole moiety in the complex could also be oxidized, which was not observed in the enzymatic systems. Therefore, the Glu189 residue in photosystem II was proposed to be protonated under the physiological condition.

1. Introduction

Phenol/phenoxyl radical, or particularly tyrosine/tyrosyl radical, redox has been a focus of increasing interest because of its involvement in many biologically important processes.[1] So far the known enzymes using this chemistry include photosynthetic systems,[2] cytochrome *c* oxidase,[3] human catalase,[4] galactose oxidase,[5] ribonucleotide reductases,[6] and so on and so forth. In different enzymes, it has been found that either the phenolic proton is hydrogen bonded with different properly oriented basic groups of the holoenzymes before oxidation,[7] or the phenoxyl radical is coordinated to different transition-metal ions after oxidation.[8] Thus, the fact that this simple redox can play such variable roles in different enzymes must be due to the different regulation effects by different chemical environments on both the rate and energetics of the phenol/phenoxyl radical transformation.[9]

For example, in photosystem II (PSII) the key player in water oxidation is proposed to be a triad composed of a multimer of chlorophylls (P_{680}), a tyrosine residue (Tyr_z, or Tyr161 of the D1 polypeptide of PSII), and a Mn cluster composed of four high-valence Mn ions.[2] (Figure 1) Upon the absorption of a photon, P_{680} is excited and transfers an electron to the pheophytin and quinone acceptor systems. This electron is finally used in the conversion of CO_2 to biomaterials. The oxidized

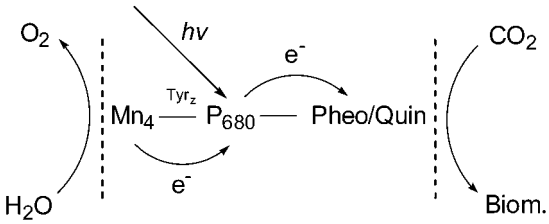

Figure 1. Schematic presentation of the main mechanism of photosystem II.

P_{680}^+, on the other hand, gets an electron from Tyr_z. The resulting $Tyr_z^\bullet$ radical is then reduced back to Tyr_z via the Mn_4 cluster by electrons ultimately derived from water.

However, detailed thermodynamic studies showed that the redox potential of the tyrosine/tyrosyl radical (from in vitro data) was far above that of P_{680}.[10] Therefore, there must be certain energy downhill interaction taking place at P_{680}^+ or Tyr_z so that the electron transfer between them can occur. This interaction was recently suggested by different experiments to be the hydrogen bonding between Tyr_z and a nearby histidine residue (His190).[2,11] Thus, oxidation of Tyr_z by P_{680}^+ is coupled with the proton transfer from hydroxyl of Tyr_z to His190, and this coupling should be one of the key factors to make the redox reaction very efficient. (Figure 2)

Theoretical studies supported the above suggestion. In 1998 Blomberg et al. on the basis of B3LYP calculations with double-ξ basis set found that hydrogen bonding between tyrosine and imidazole lowered the redox potential of tyrosine by 25.6 kcal/mol.[12] At the same time, O'Malley performed DFT B3LYP calculations with EPR-II, double-ξ basis set, and showed that

* Authors to whom correspondence should be addressed. E-mail (Liu): leiliu@chem.columbia.edu. E-mail (Guo): qxguo@ustc.edu.cn.

† Current address: Department of Chemistry, Columbia University, New York, NY 10027.

‡ Current address: Department of Chemistry, Wayne State University, Detroit, MI 48202.

10.1021/jp014425z CCC: $22.00
Published on Web 04/10/2002

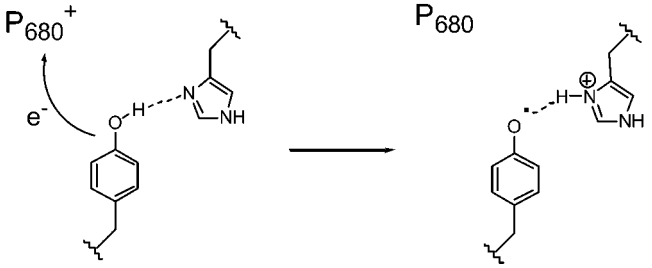

Figure 2. Schematic presentation of the His190 assisted proton-coupled electron transfer from Tyr_z to $P_{680}+$ in PSII.

one-electron oxidation of a phenol−imidazole hydrogen-bonded complex could lead to spontaneous transfer of the phenolic proton to imidazole.[13] All these findings were also reproduced recently by Eriksson et al. at B3LYP/6-311+g(2df, p)//6-31 g** level of calculations.[14]

The above proton-coupled electron transfer has also been found in nonenzymatic chemistry. In 1999, Styring et al. made a ruthenium tris-bipyridyl complex covalently linked to L-tyrosine with basic substituents.[15] It was found that the electron transfer from the substituted tyrosine to the ruthenium part was at least 2 orders of magnitude greater than that in the similar compound without any basic substituent attached to tyrosine. Therefore, the hydrogen bonding between the basic substituent and tyrosine was proposed to be responsible for the fast electron transfer, which mimicked the proposed His190-Tyr_z interaction in PSII. Similarly, Matsumura et al. attached different basic amine groups to phenols recently.[16] They found that those phenols capable of forming intramolecular hydrogen bonds could be oxidized to persistent phenoxyl radicals in solution. It was also found that the intramolecular hydrogen bonding could dramatically change the phenol redox potential.

In the present study, we systematically investigated the effects of hydrogen bonding to various amines on the redox reactions of phenol. Not only the biologically related imidazole but also other types of amines were considered. Also, we not only investigated the hydrogen bonding effects on the redox potential of phenol, but also studied the strengths and properties of the hydrogen bonds between phenol/phenoxyl radical and amines. Similar studies on the effects of hydrogen bonding on the properties (e.g. isotropic hyperfine coupling constants) of radicals have been conducted before,[17] but our major concern was the effects of intermolecular noncovalent interactions on the redox potential.

2. Methods

All the calculations were performed with GAUSSIAN 98.[18] In the geometry optimization (U)B3LYP/6-31+g* method was used, because it is well-known that this method can provide accurate electronic structures and properties of various molecules and radicals at reasonable computational cost. In fact, recent studies even showed that the accuracy of B3LYP in the geometry optimization and frequency calculations is roughly comparable, or better, to CCSD method and therefore is a good compromise between cost and accuracy for the study of molecular radicals.[19] By contrast, Hartree−Fock and MP2 methods, either restricted open-shell or unrestricted, work in a much less reliable way for the geometry optimization of radicals.[19] In our (U)B3LYP/6-31+g* geometry optimization no constraint was employed, and all the optimized structures were confirmed by (U)B3LYP/6-31+g* frequency calculations to be real minima.

The total energies of the species were calculated at RMP2/6-311++g** level using (U)B3LYP/6-31+g* geometries. They were corrected with zero-point energies obtained at (U)B3LYP/6-31+g* level (unscaled). Here, selection of the MP2 instead of the (U)B3LYP method was based on the consideration that use of the DFT method to calculate the energetics of weak molecular complexes is possibly not as good as use of perturbation methods, because none of the existing DFT functionals describe the London dispersion energy.[20] Also, as it has been known that UMP2 method is usually associated with high spin contamination for radicals, the RMP2 method was used for the single-point energy calculations throughout this study. In addition, it has also been shown by Radom et al. that RMP2 calculations usually could fairly well predict the energies of radicals, whereas the (U)B3LYP method tends to overestimate the radical stabilization energies.[21]

The hydrogen bonding energy was calculated from the difference between the total energy of the complex and the sum of the total energies of the corresponding monomers at RMP2/6-311++g** level. This interaction energy was corrected with the (U)B3LYP/6-31+g* zero-point energies (unscaled) as well as the basis set superposition error (BSSE) estimated with the full counterpoise procedure at the RMP2/6-311++g** level.[22]

The proton affinities of a species A were calculated as the enthalpy change of the following chemical reaction at 298 K in the gas phase:

$$A + H^+ \rightarrow AH^+ \qquad (1)$$

The RMP2/6-311++g**//(U)B3LYP/6-31+g* method was used, and zero-point energies, finite temperature (0−298 K) correction, and the pressure−volume work term were all taken into account in the calculations of proton affinities.

3. Results and Discussion

3.1. Effects of the Basis Sets on Geometry Optimization. With the smallest phenol−ammonia system, we were able to use various basis sets to examine the effects of the basis sets on geometry optimization. The results are listed in Table 1.

According to Table 1, it can be seen that basis set effects on geometry optimization of the phenol−ammonia complex are very small. In particular, the O−H bond lengths predicted by different methods are never over 0.01 Å different from each other. Also, the N−H nonbonding distances are in ±0.05 Å of agreement with each other, and the variation of the O−H−N angle is less than 3 degree.

In comparison, basis set effects on geometry optimization of the phenoxyl radical−ammonium complex are slightly larger. In detail, the N−H bond lengths can change about 0.03 Å when different basis sets are used. The variation of O−H nonbonding distance is about 0.09 Å, and the variation of O−H−N angle is about 3 degrees.

The adiabatic ionization potentials of the phenol−ammonia complex to phenoxyl radical−ammonium complex, calculated as ($E_{\text{radical complex}} - E_{\text{phenol complex}}$) also shows small changes when different basis sets are used. In particular, it could be noticed that the basis sets without diffusion functions (6-31 g*, 6-311 g*) predict significantly lower ionization potentials than other ones. In comparison, simple addition of diffusion functions (6-31+g*, 6-311+g*) effectively improves this estimation, whose values are only about 0.2 eV smaller than the values predicted by considerably larger basis sets.

On the basis of the above results, we expected that (U)-B3LYP/6-31+g* optimization should represent a good compromise between the accuracy and CPU-cost of the amount of calculation with our DELL 6400 station. Our choice of the

TABLE 1: Geometries and Energies of the Phenol−Ammonia and Phenoxyl Radical−Ammonium Complexes Optimized by the (U)B3LYP Method with Different Basis Sets

	phenol−ammonia				phenoxyl radical-ammonium				
basis set	O−H (Å)	N−H (Å)	∠O−H−N (deg)	*E* (a.u.)	O−H (Å)	N−H (Å)	∠O−H−N (deg)	*E* (a.u.)	ΔE^a (eV)
6-31 g*	0.993	1.837	169.96	−364.0	1.497	1.108	165.11	−363.8	7.00
6-31+g*	0.992	1.856	169.54	−364.1	1.542	1.088	165.58	−363.8	7.26
6-311 g*	0.986	1.837	171.30	−364.1	1.544	1.083	164.77	−363.9	7.16
6-311+g*	0.986	1.862	169.42	−364.1	1.561	1.074	166.19	−363.9	7.25
6-311++g**	0.984	1.882	168.68	−364.2	1.500	1.094	166.44	−363.9	7.39
6-311++g(2df,p)	0.984	1.887	168.66	−364.2	1.482	1.102	167.10	−363.9	7.41
6-311++g(3d,3p)	0.983	1.887	168.86	−364.2	1.486	1.100	166.99	−363.9	7.41
Aug-cc-pVDZ	0.986	1.872	169.59	−364.1	1.472	1.108	166.65	−363.8	7.41

[a] Adiabatic ionization potentials of the phenol−ammonia complex to phenoxyl radical−ammonium complex, calculated as ($E_{\text{radical complex}} - E_{\text{phenol complex}}$). These values were corrected by ZPEs calculated at the (U)B3LYP/6-31+g* level (unscaled).

TABLE 2: RMP2 Energies (kcal/mol) of Phenol−Ammonia and Phenoxyl Radical−Ammonium Complexes Obtained with Different Basis Sets Using (U)B3LYP/6-31+g* Geometries

	phenol−ammonia		phenoxyl radical−ammonium		
basis set	E_{total} (a.u.)	$\Delta E_{\text{complex}}$ (kcal/mol)	E_{total} (a.u.)	$\Delta E_{\text{complex}}{}^a$ (kcal/mol)	$\Delta E_{\text{oxidation}}{}^b$ (eV)
6-31 g*	−362.9	−7.3	−362.6	−33.4	7.10
6-31+g*	−362.9	−6.2	−362.6	−31.6	7.10
6-311 g*	−363.0	−6.7	−362.7	−31.0	7.00
6-311+g*	−363.0	−6.5	−362.8	−30.3	7.10
6-311++g**	−363.1	−5.9	−362.8	−32.1	7.40
6-311++g(2df,p)	−363.3	−6.4	−363.0	−26.6	7.51
6-311++g(3d,3p)	−363.2	−6.3	−362.9	−26.7	7.52
Aug-cc-pVDZ	−363.0	−6.2	−362.8	−26.8	7.47

[a] The interaction energy calculated at one level of theory was corrected by BSSE calculated at the same level of theory and ZPE calculated at the (U)B3LYP/6-31+g* level (unscaled). [b] Adiabatic ionization potentials of the phenol−ammonia complex to the phenoxyl radical−ammonium complex, calculated as ($E_{\text{radical cation}} - E_{\text{phenol complex}}$). These values were corrected by ZPEs calculated at the (U)B3LYP/6-31+g* level (unscaled).

6-31+g* basis set in optimization was also made on the basis of Hobza's finding that use of the 6-31+g* basis set could lead to fairly accurate values of polarizability and the quadrupole moment of benzene.[23]

3.2. Effects of the Basis Sets on Single-Point Energy Calculation. With the same phenol−ammonia case, we were also able to examine the basis sets on the single-point energy calculations with the RMP2 method. The corresponding results are summarized in Table 2.

From Table 2, it can be seen that the basis set effects on the energy calculations are not negligible. In particular, comparison of the energies calculated with the 6-31 g* basis set and calculated with 6-311++g(3d,3p) or Aug-cc-pVDZ ones reveals differences of about 1∼7 kcal/mol in binding energy and of about 0.4 eV in ionization potential.

Nevertheless, it can be seen that the energies calculated at 6-311++g** level are closer to those calculated with much larger basis sets. This is especially true for ionization potential: the RMP2/6-311++g** predicts a value of 7.40 eV, whereas 6-311++g(3d,3p) and Aug-cc-pVDZ predict values of 7.52 and 7.47 eV, respectively. Therefore, we expected that use of RMP2/6-311++g** method in the single-point energy calculations was efficient as well as reliable.

Interestingly, it could be noticed that the (U)B3LYP/Aug-cc-pVDZ//(U)B3LYP/ Aug-cc-pVDZ method predicts a value of 7.41 eV for the ionization potential of the phenol−ammonia system. This value is very close to that predicted by the RMP2/Aug-cc-pVDZ// (U)B3LYP/6-31+g* method, namely, 7.47 eV. This again shows that optimization with the (U)B3LYP/6-31+g* method is reasonably good.

3.3. Effects of Hydrogen Bonding to Ammonia on Phenol Oxidation. As several theoretical[24−26] as well as experimental[27] studies have been done on the phenol−ammonia complex and its oxidation, we would like to investigate this system in detail at first and compare our results with previous ones.

According to Table 3, in the free phenol molecule the O−H bond length is 0.970 Å at the B3LYP/6-31+g* level, which is very close to the previous value (0.968 Å at the B3LYP/D95++** level).[24] This bond will be elongated to 0.992 Å (or 0.991 Å according to ref 24) in the phenol−ammonia complex. After oxidation, the O−H bond length in the free phenoxyl radical cation is 0.979 Å (0.977 Å in ref 24), which is completely different from the corresponding value, 1.542 Å (1.475 Å in ref 24, and 1.603 Å at CASSCF/6-31+g** level in ref 25) found in the phenoxyl radical−ammonium complex. Therefore, oxidation of phenol results in a proton transfer from phenol to ammonia. This proton transfer should also be barrierless as neither a nonproton-transferred phenol radical cation−ammonia complex nor a transition state structure for the proton transfer between phenol and ammonia could be found by us on the potential energy surface with B3LYP/6-31+g* method. This barrierless proton transfer was also proposed in previous studies on the basis of UHF/6-31+g*,[26] B3LYP/D95++**,[24] and CASPT2/6-31+g**[25] calculations.

The energetic effect of the proton transfer on phenol oxidation is significant, too. As shown in Table 4, the free phenol has an adiabatic ionization potential of 8.41 eV (8.16 eV in ref 13) in the gas phase. When complexed to ammonia, this ionization potential changes to 7.40 eV (7.33 eV in ref 24 at the B3LYP/D95++** level), which represents a 1.01 eV shift from the original value. It means that phenol will be much easier to oxidize when complexed to ammonia. Further calculations reveal that the phenol−ammonia complex has a binding energy of 5.9 kcal/mol (7.8 kcal/mol in ref 24 at the B3LYP/D95++** level),

TABLE 3: Optimal Geometries of Different Phenol and Phenoxyl Radical Complexes optimized at the (U)B3LYP/6-31+g* Level

	phenol complexes			phenoxyl radical complexes (the proton is on N)			phenoxyl radical cation complexes (the proton is on O)		
amine	O−H (Å)	N−H (Å)	∠O−H−N (deg)	O−H (Å)	N−H (Å)	∠O−H−N (deg)	O−H (Å)	N−H (Å)	∠O−H−N (deg)
(with no base)	0.970						0.979		
NH_3	0.992	1.856	169.54	1.542	1.088	165.58			
CH_3NH_2	0.996	1.832	169.14	1.619	1.064	164.15			
imidazole	0.990	1.862	173.22	1.649	1.051	170.96			
imidazole + formate	1.017	1.703	176.61	1.908	1.022	177.85	0.988	1.873	172.09
imidazole + formic acid	0.994	1.832	173.82	1.703	1.041	164.13			
NH_2F	0.981	1.972	167.77				1.033	1.663	173.90
NF_3	0.971	2.402	165.92				0.989	2.014	171.80
NH_2CCH	0.981	1.988	163.43				1.043	1.637	170.46
NH_2CCCH_3	0.984	1.956	164.21	1.487	1.111	166.47	1.071	1.548	170.68
NH_2CCNO_2	0.974	2.147	158.13				1.013	1.792	170.34
NH_2CCF	0.982	1.973	163.45	1.416	1.143	166.74	1.052	1.607	169.91
NH_2CCOH	0.983	1.966	163.92	1.460	1.123	167.94	1.062	1.575	170.94
NH_2CCCl	0.982	1.988	163.72	1.426	1.139	166.63	1.048	1.622	170.26
$NH_2C_6H_4F$	0.986	1.927	163.92	1.598	1.073	167.94			

TABLE 4: Energetics of the Phenol/Phenoxyl Radical Oxidation with the Presence of Various Amines Calculated at the RMP2/6-311++g//(U)B3LYP/6-31+g* Level**

	phenol complex		phenoxyl radical complex (the proton is on N)			phenoxyl radical cation complex (the proton is on O)		
amine	E_{total} (a.u.)	$\Delta E_{complex}$[a] (kcal/mol)	E_{total} (a.u.)	$\Delta E_{complex}$[a] (kcal/mol)	$\Delta E_{oxidation}$[b] (eV)	E_{total} (a.u.)	$\Delta E_{complex}$[a] (kcal/mol)	$\Delta E_{oxidation}$[b] (eV)
(with no base)	−306.7					−306.4		8.41
NH_3	−363.1	5.9	−362.8	32.1	7.40			
CH_3NH_2	−402.3	7.2	−402.0	29.4	7.21			
imidazole	−532.3	8.5	−532.1	25.9	7.02			
imidazole + formate	−721.2	17.2	−721.1	13.2	3.44	−721.0	118.8	4.00
imidazole + formic acid	−721.7	9.8	−721.5	23.5	6.52			
NH_2F	−462.1	4.5				−461.8	18.6	7.83
NF_3	−660.1	0.4				−659.8	1.2	8.33
NH_2CCH	−439.0	4.9				−438.7	18.3	7.81
NH_2CCCH_3	−478.2	5.3	−477.9	32.4	7.64	−477.9	23.0	7.66
NH_2CCNO_2	−643.1	2.9				−642.8	9.9	8.11
NH_2CCF	−538.1	4.5	−537.8	35.0	7.91	−537.8	18.1	7.82
NH_2CCOH	−514.1	5.4	−513.8	32.9	7.71	−513.8	23.0	7.64
NH_2CCCl	−898.1	4.5	−897.8	34.2	7.82	−897.8	18.6	7.80
$NH_2C_6H_4F$	−692.6	6.3	−692.3	29.3	7.53			

[a] The interaction energy was BSSE (at RMP2/6-311++g** level) and ZPE (at (U)B3LYP/6-31+g* level, unscaled) corrected. [b] Adiabatic ionization potentials of phenol−ammonia complex to phenoxyl radical−ammonium complex, calculated as ($E_{radical\ complex} - E_{phenol\ complex}$). These values were corrected by ZPEs calculated at the (U)B3LYP/6-31+g* level (unscaled).

which is much smaller than the corresponding value, 32.1 kcal/mol (32.2 kcal/mol in ref 24 at the B3LYP/D95++** level) for the phenoxyl radical−ammonium complex.

3.4. Effects of Hydrogen Bonding to Other Amines on Phenol Oxidation. In Table 3 and Table 4 are summarized the geometry (Figure 3) and energetics of the complexes between the phenol/phenoxyl radical and a number of other amines. For every complex both the proton-transferred structure (i.e., the proton is on N) and the nonproton-transferred structure (i.e., the proton is on O) are considered in the geometry optimization, but in the tables we reported only the structures corresponding to the real minima on the (U)B3LYP/6-31+g* potential surfaces.

According to the tables, it can be seen at first that proton transfer does not occur in all the non-oxidized phenol−amine complexes, which agrees with the previous findings.[28] However, in the oxidized complexes, depending on the properties of the amines, the proton-transfer either occurs in a barrierless manner or occurs but with a certain energy barrier, or never takes place at all.

For the oxidized phenol−methylamine system, only the proton-transferred complex is found to be a real minimum. Therefore, this oxidation should also involve a proton-coupled electron transfer. Compared to 7.40 eV of oxidation potential for the phenol−ammonia complex, the oxidation potential of phenol−methylamine system is found to be 7.21 eV, 1.20 eV lower than that of free phenol. This larger lowering effect of methylamine compared to ammonia is expected, because methyl is an electron-donating group.

By contrast, when the amine is fluorinated, the resulting phenol−fluoroamine system cannot transfer the proton during the course of oxidation, because only one minimum corresponding to the nonproton-transferred structure can be found for the oxidized complex. Here the oxidation potential is found to be 7.83 eV, only 0.58 eV lower than that of free phenol. In addition, when the amine is triply fluorinated, only the nonproton-transferred structure is found to be the real minimum for the oxidized pheno−-trifluoroamine complex, too. The corresponding oxidation potential is 8.33 eV, which is very close to 8.41 eV found for free phenol.

In close relation to the biological tyrosine oxidation, the phenol−imidazole systems are the most interesting. Here, it is found that for the oxidized phenol−imidazole complex, only one minimum corresponding to a proton-transferred structure can be found. This is in agreement with the results from previous

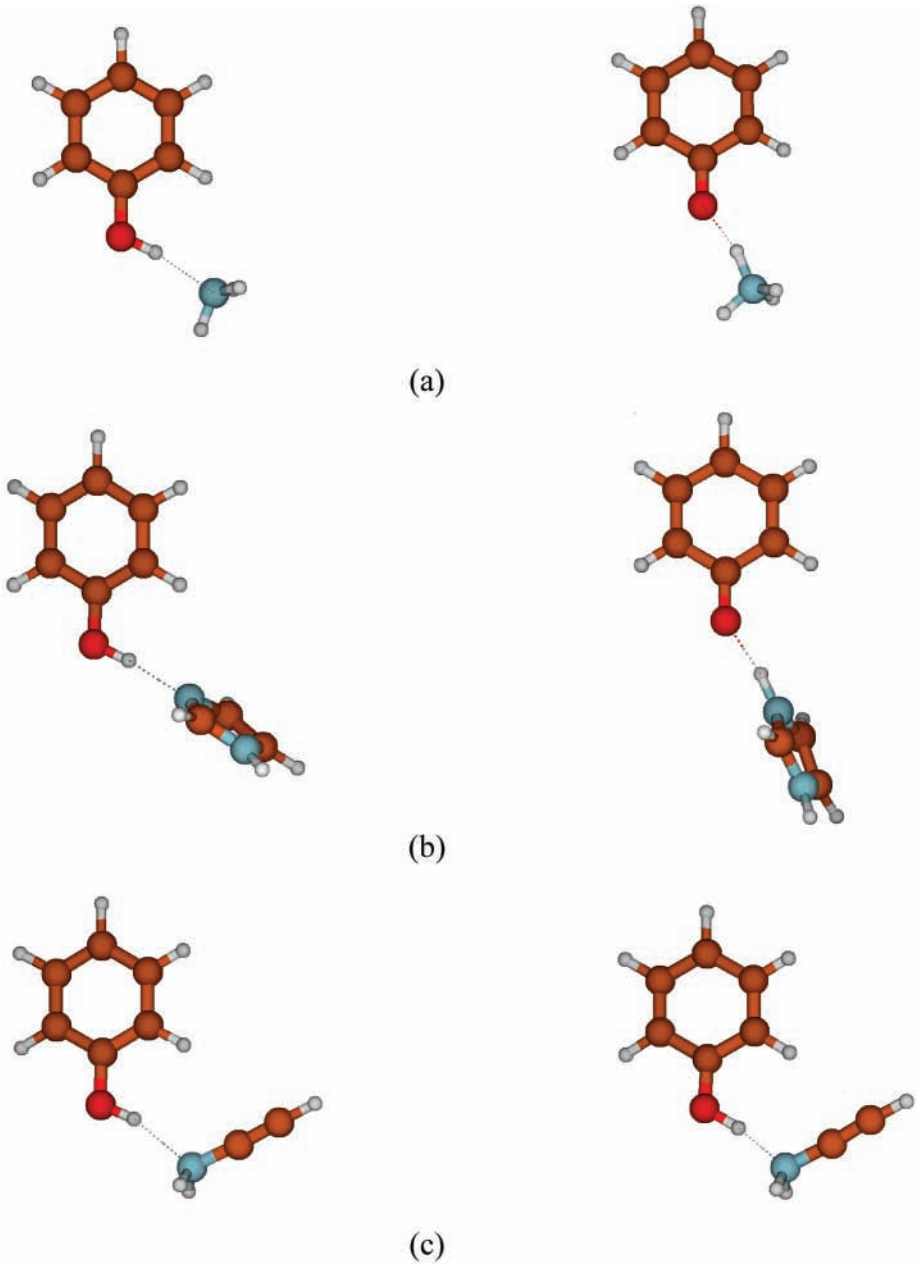

Figure 3. The (U)B3LYP/6-31+g* optimized structures of (a) phenol−ammonia complex and phenoxyl radical−ammonium complex, (b) phenol−imidazole complex and phenoxyl−imidazolium complex, and (c) phenol−aminoacetylene complex and phenoxyl radical cation−aminoacetylene complex.

calculations.[13,14] The corresponding adiabatic oxidation potential, 7.02 eV, is a little higher than the previously predicted one, 6.65 eV.[13]

As recently it was suggested from the experimental studies that in addition to His190, Glu189 of the D1 polypeptide of PSII is also possibly involved in the hydrogen bonding to Tyr_z,[29] we also calculated the oxidation of phenol−imidazole−formate system. Remarkably, it is found that such a system has an oxidation potential of 3.44 eV (or 4.00 eV if no proton transfer occurs), which is much lower than that of free phenol. For the corresponding oxidized complex, both the proton-transferred or nonproton-transferred structures are found to be real minima. The reason for the double minima remains to be clarified, because intuitionally formate should make imidazole more basic and therefore, proton transfer should be easier to take place than that observed for the phenol−imidazole complex. Nevertheless, it should be mentioned that the original proton on imidazole is always transferred to formate after the system is oxidized.

Since the above oxidation potential is too low, it appears to us that the carboxylate−midazole salt bridge may not correspond to the real situation in PSII. Therefore, we also used formic acid to interact with imidazole, which results in a phenol−imidazole−formic acid triad. Such a system is found to have an oxidation potential of 6.52 eV, which is 1.89 eV lower than that of free phenol. Interestingly, here we are only able to find one minimum for the oxidized complex, which corresponds to the proton-transferred structure. It should be mentioned that a decrease of 1.89 eV appears much more reasonable for the enzymatic system than a decrease of 4.97 eV found for the phenol−imidazole−formate system. Therefore, one can propose that if Glu189 is involved in the hydrogen bonding systems of PSII, it must remain protonated at neutral pH values. Indeed, from very recent experimental studies Debus et al. also proposed the unprotonated state of Glu189 in PSII.[30] The driving force for this unusual unprotonation is possibly the interaction of Glu189 with nearby charged groups in the enzyme.[30]

TABLE 5: Proton Affinities of the Amines Calculated at the RMP2/6-311++G//B3LYP/6-31+g* Level of Theory**

amine	H···N distance in the protonated complex (Å)	proton affinity (kcal/mol)
phenoxyl radical	0.979	−206.7
phenol anion	0.970	−347.6
NH_3	1.029	−204.4
CH_3NH_2	1.028	−214.9
imidazole	1.016	−223.3
imidazole + formate	1.011	−326.1
imidazole + formic acid	1.014	−236.8
NH_2F	1.034	−182.0
NF_3	1.048	−131.1
NH_2CCH	1.035	−189.1
NH_2CCCH_3	1.034	−197.3
NH_2CCNO_2	1.036	−172.7
NH_2CCF	1.034	−189.7
NH_2CCOH	1.034	−197.1
NH_2CCCl	1.035	−190.6
$NH_2C_6H_4F$	1.029	−206.4

Having studied several typical amines, we were next interested to know the substituent effects on the phenol−amine oxidation. Apparently the best systems to study such substituent effects are phenol−*para*-aniline complexes. However, after trying several substituents, we were only able to get one stable complex of phenoxyl radical/radical cation with 4-fluoroaniline. This is mainly caused by the ortho proton of anilines, which can form a C−H···O hydrogen bond to phenol/phenoxyl and consequently makes the potential surface very complicated. Nevertheless, in the 4-fluoroaniline case, only the proton-transferred structure is found to be the real minimum (and the only one minimum) for the oxidized complex. The corresponding oxidation potential is 7.53 eV, which is 0.88 eV lower than that of free phenol.

Thus, we changed to use substituted aminoacetylenes to study the substituent effects on phenol−amine oxidation. As no ortho proton is involved here, the geometry optimization can be smoothly done.

From Tables 3 and 4, it can be seen that $NH_2-C\equiv C-H$ results in a nonproton-transferred structure for the oxidized complex only. The corresponding oxidation potential is 7.81 eV. Similar behavior is also found for $NH_2-C\equiv C-NO_2$, whose oxidation potential is relatively higher, namely, 8.11 eV. However, with the electron-donating substituent including F, CH_3, OH, and Cl, both the proton transferred and nonproton-transferred structures are found to be real minima for the oxidized phenol−aminoacetylene complexes. Their corresponding oxidation potentials are also lower than that found for the phenol complex of $NH_2-C\equiv C-H$.

3.5. Structure−Reactivity Relationship in the Amine Effects on Phenol Oxidation. Before we discuss the structure−reactivity relationship in the amine effects on phenol oxidation, we would like to know the basicities of the amines which can be well reflected by their gas-phase proton affinities.

Thus we calculated the proton affinities of the amines using the standard procedure at RMP2/6-311++g**//(U)B3LYP/6-31+g* level. The corresponding values are listed in Table 5. It should be mentioned that the above level of calculation appears to be adequate, because our calculated proton affinity for NH_3 is −204.4 kcal/mol compared to the recent experimental value −204.0 kcal/mol.[31] In addition, our calculated proton affinity for phenoxyl radical is −206.7 kcal/mol compared to the recently reported value −208.7 kcal/mol.[31]

It then turns out that most of the amine effects on the phenol/phenoxyl oxidation can be explained by using the calculated proton affinities. First of all, as phenol anion has a proton affinity of −347.6 kcal/mol, which is much lower than the proton affinities of all the amines, it is understandable that no proton transfer can occur in the neutral phenol−amine complexes. By contrast, the proton affinity of the phenoxyl radical is very close to the proton affinities of amines, so that proton transfer from the phenoxyl radical cation to the amine is possible. It should be mentioned that the large difference in the proton affinity between the phenol anion and the phenoxyl radical can also be used to explain the amine effect on phenol oxidation. In detail, as the phenoxyl radical has a smaller proton affinity than the phenol anion, the phenoxyl radical cation is more acidic than phenol. This means that phenol−amine interaction is less strong than the phenoxyl radical cation−amine interaction. Thus, the fact that amine can stabilize the oxidation product (phenoxyl radical cation) better than the starting material (phenol) should clearly be able to lower the free energy change and therefore, oxidation potential of phenol oxidation.

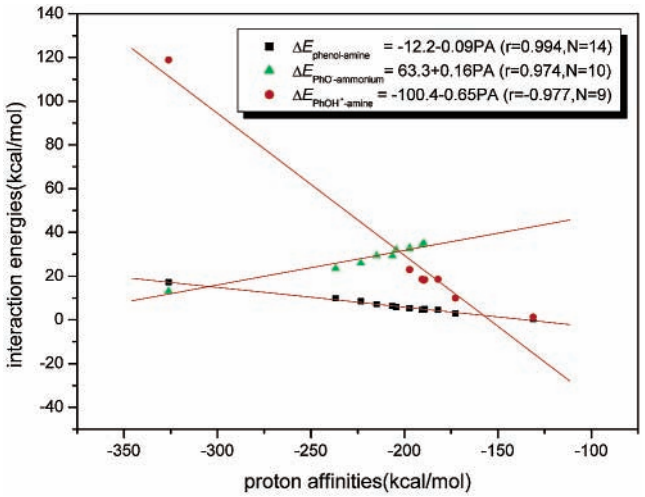

Figure 4. The dependence of the phenol−amine, phenoxyl radical−ammonium, and phenoxyl radical cation−amine interaction energies on the proton affinities of the amines.

Interestingly, for those oxidized complexes where only the proton-transferred structure is found to be minimum, the absolute proton affinities of the amines (NH_3, NH_2CH_3, imidazole, imidazole−formic acid, and $NH_2C_6H_4F$) are larger than 204.4 kcal/mol, compared to the absolute proton affinity of the phenoxyl radical 206.7 kcal/mol. When both the proton-transferred and nonproton-transferred structures are found to be minima, the absolute proton affinities of the amines (NH_2CCCH_3, NH_2CCF, NH_2CCOH, and NH_2CCCl) are located in the range of 189.7−197.3 kcal/mol. When only the nonproton-transferred structure is found to be minimum, the absolute proton affinities of the amines (NH_2F, NF_3, NH_2CCH, and NH_2CCNO_2) are smaller than 189.1 kcal/mol. Thus, the proton affinity of the amine should determine the shape of the potential surface of the oxidized phenol−amine complex. The only exception to the above empirical rules is the phenol−imidazole−formate system, whose reason remains to be clarified.

Another interesting properties involved in phenol−amine oxidation that can be related to the proton affinities of the amines are the noncovalent interaction energies between phenol/phenoxyl radical and amines. In detail, plotting the interaction energies of the phenol−amine, phenoxyl radical cation−amine, or phenoxyl radical−ammonium complexes versus the proton affinities of the corresponding amines gives three straight lines. (Figure 4) The absolute correlation coefficients are 0.994, 0.977, and 0.974, respectively, which means that each correlation is

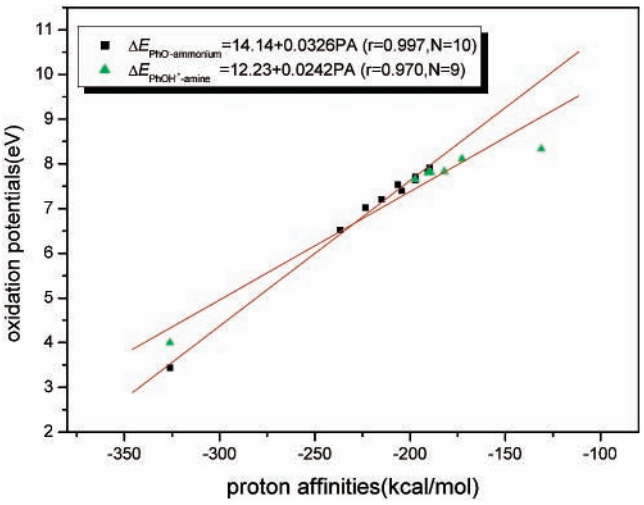

Figure 5. The dependence of the oxidation potentials of the phenol−amine systems on the proton affinities of the amines.

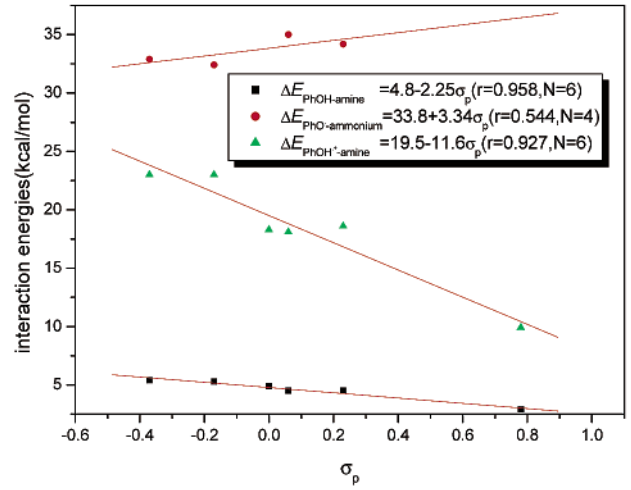

Figure 6. The dependence of the phenol−amine, phenoxyl radical−ammonium, and phenoxyl radical cation−amine interaction energies on the substituent σ_p constants for the substituted phenol−aminoacetylene systems.

very strong. Therefore, the ability of the amine to bind with phenol/phenoxyl radical is parallel to the ability of the same amine to bind with a proton.

Similarly, the oxidation potentials of the phenol−amine complexes are also dependent on the proton affinities of the corresponding amines. As shown in Figure 5, a decrease of absolute value of the proton affinity results in an increase of the oxidation potential not only for the proton-transferred systems but also for the nonproton-transferred systems. The correlation coefficients are 0.941 and 0.995, respectively. Therefore, the extents to which an amine can shift the oxidation potential of phenol are also highly predictable.

3.6. Hammett Correlations. For the several substituted aminoacetylenes, it turns out that not only the proton affinities of the amines but also the Hammett σ_p constants[32] of the substituent can also be used to predict the energetics in the phenol−amine oxidation.

As shown in Figure 6, the plots of the interaction energies of the phenol−amine, phenoxyl radical−ammonium, and phenoxyl radical cation−amine complexes versus the substituent Hammett σ_p constants are linear. The correlation coefficients are 0.958, 0.544, and 0.927, respectively. It should be mentioned that the correlation coefficient for the phenoxyl radical−ammonium system is low (0.544), clearly because in the system ammonium is not able to have any conjugation with the substituent. Such a behavior, on the other hand, clearly indicates that in the phenol−amine and phenoxyl radical cation−amine complexes the amino group still has normal conjugation with the substituent and therefore, the assignment of the proton completely to the phenol side is correct.

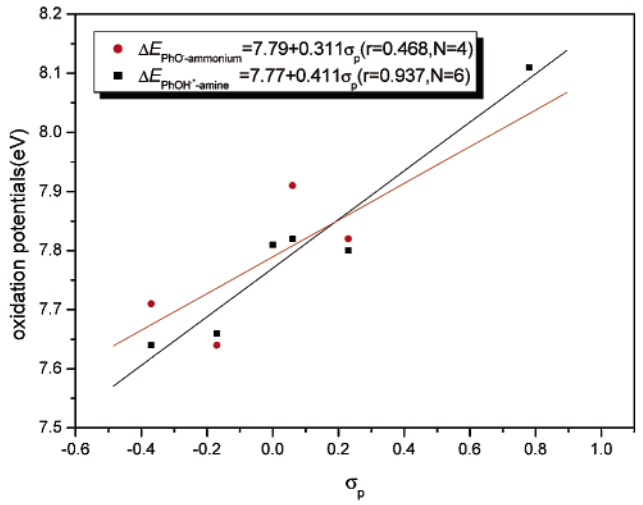

Figure 7. The dependence of the oxidation potentials on the substituent σ_p constants on the phenol−aminoacetylene systems.

Correlation of the oxidation potentials of the phenol−aminoacetylene complexes with the substituent Hammett σ_p constants shows similar behaviors. Thus, without proton transfer, the correlation between the oxidation potential and the substituent Hammett σ_p constants is good ($r = 0.937$). By contrast, when a proton transfers the correlation between the same two variables is poor ($r = 0.468$). Again, the Hammett type correlation can clearly show the position of the proton in the oxidized complexes.

3.7. Spin Densities. Spin density distribution is important for understanding organic radicals. Therefore we calculated the spin density distributions for all the systems using RMP2/6-311++g** populations. The typical spin density distributions for different types of phenoxyl−amine complexes are shown in Figure 8.

From Figure 8, it can be seen that in the phenoxyl radical most of the spin is located on the phenolic oxygen. All the carbons also carry some spin densities, but the amounts are small. This distribution is in sharp contrast to that found for the phenoxyl radical cation, where the phenolic oxygen carries little spin densities. Most of the spin densities of the phenoxyl radical cation are actually located on C1 and C4 positions.

Interestingly, in the phenoxyl radical−ammonium complex the spin density distribution is also completely different from that found for the free phenoxyl radical. Unlike the isolated phenoxyl radical, the phenolic oxygen in the complex does not carry most of the spin density. On the other hand, C1, C2, C6, and especially C4 of phenol in the complex carry significant amounts of spin densities, which is again different from that found for free phenoxyl radical. It should also be mentioned that the ammonium moiety does not carry any significant amount of spin in the complex. Thus, instead of sharing any spin density with the phenoxyl radical, the role of ammonium is mainly to delocalize the spin from the phenolic oxygen to the rest of the phenol molecule. As known, such a spin delocalization should always lower the total energy of a radical system.[33] This energy lowering effect can also be used to explain the decrease of the

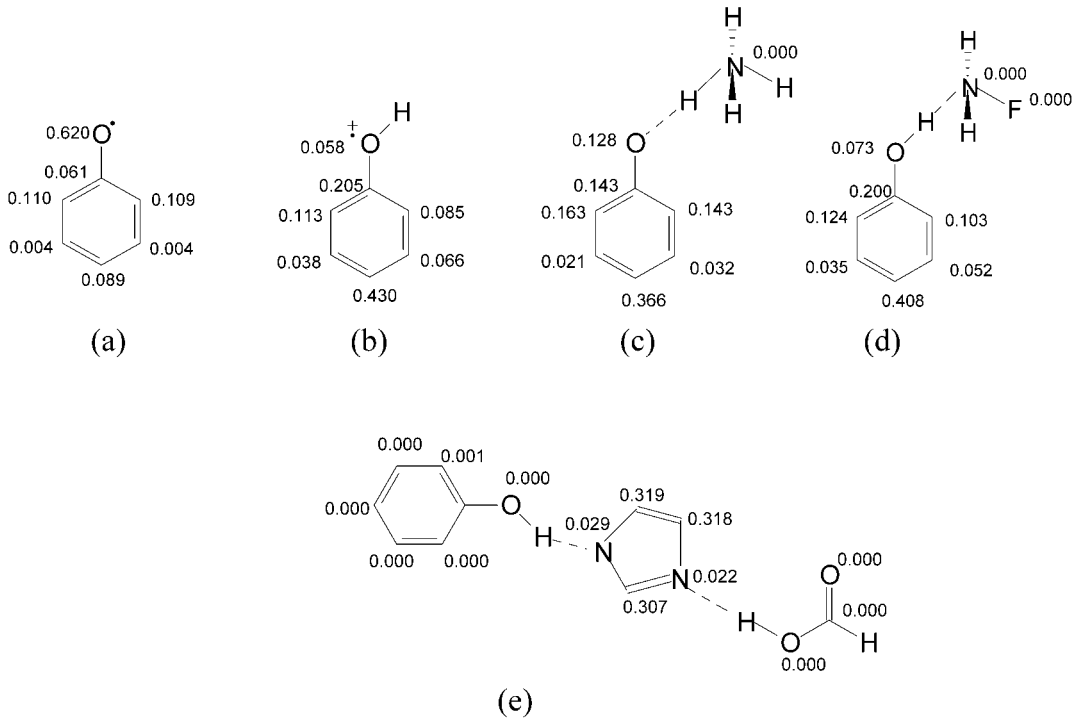

Figure 8. The spin densities in (a) free phenoxyl radical, (b) phenoxyl radical cation, (c) phenoxylammonium complex, (d) phenoxyl radical cation−NH_2F complex, and (e) phenoxyl radical cation−imidazole−formate complex from RMP2/6-311++g** population.

oxidation potential of phenol caused by the hydrogen bonding to ammonia.

Nevertheless, it can be seen from Figure 8 that the spin density distribution in the phenoxyl radical cation−NH_2F complex is almost the same as that found for the free phenoxyl radical cation. No spin density is transferred to the NH_2F moiety. These observations are consistent with the fact that the effects of NH_2F on phenol oxidation are small.

It should be mentioned that the spin density distribution of the nonproton-transferred oxidized phenol−imidazole−formate complex explains why this structure is a minimum in addition to its corresponding proton-transferred structure. As shown in Figure 8, interestingly there is almost no spin density localized on either the phenol part or the formate part in the complex. Instead, nearly all the spin is distributed on the imidazole moiety, or more precisely, the three carbons of imidazole. Thus, unlike the other nonproton-transferred oxidized phenol−amine complexes which can actually be regarded as the phenoxyl radical cation−amine complexes, the nonproton-transferred oxidized phenol−imidazole−formate complex should be regarded as the complex of a neutral phenol molecule, an imidazole radical cation, and a neutral formic acid molecule. The reason for the formation of the imidazole radical cation is presumably the strong electron-donating effect of formate anion in the nonoxidized complex. Therefore, unlike phenol−imidazole or phenol−imidazole−formic acid complexes, the phenol−imidazole−formate complex should have two minima after oxidation. One of the two minima does not correspond to phenol oxidation, but to imidazole oxidation. This is not the case observed for the enzymes, and therefore probably the Glu189 residue in PSII should be protonated under physiological conditions.[30]

The above results concerning the imidazole−formate complexes are also supported by the molecular orbital analyses. As shown in Figure 9, the SOMO (singly occupied molecular orbital) of the phenol radical cation−midazole−formic acid complex is mostly populated on the phenol moiety of the complex. By contrast, the SOMO of the phenol radical cation−imidazole−formate complex is mainly populated on the imidazole moiety of the complex. Therefore, the formic acid complex can be regarded as a normal phenol radical, whereas the formate complex has to be regarded as an imidazole radical. Clearly, the latter is not what we want.

For other complexes, as the observed spin density distributions are basically the same as those found for the above several typical cases, we simply list the spin densities of the phenolic oxygens of the complexes in Table 6. From Table 6, it can be seen that for the proton-transferred phenoxyl radical−ammonium complexes, the spin density at phenolic oxygen is significantly lower than that found for free phenoxyl radical, indicating a strong spin delocalization effect exerted by the amines. By contrast, the spin density at the phenolic oxygen found for the nonproton-transferred phenoxyl radical cation−amine complexes is almost the same as that found for the free phenoxyl radical cation, indicating small effects of the corresponding amines on phenol oxidation. The only exception here is the phenol−imidazole−formate complex, whose oxidation actually occurs at imidazole instead of phenol.

4. Conclusion

In the present study we performed RMP2/6-311++g**//(U)-B3LYP/6-31+g* studies about the amine effects on the phenol oxidation. The several important findings from the study include the following:

(1) The basis set effects on the calculations are not large. Geometry optimization using the (U)B3LYP method with moderate basis sets can afford reasonably good structures. Single-point calculations at RMP2 level with the 6-311 g basis set augmented with appropriate polarization and diffusion functions can give fairly accurate energies.

(2) Hydrogen bonding to ammonia can significantly affect the oxidation of phenol. The oxidation process actually corresponds to a barrierless proton-coupled electron transfer. The

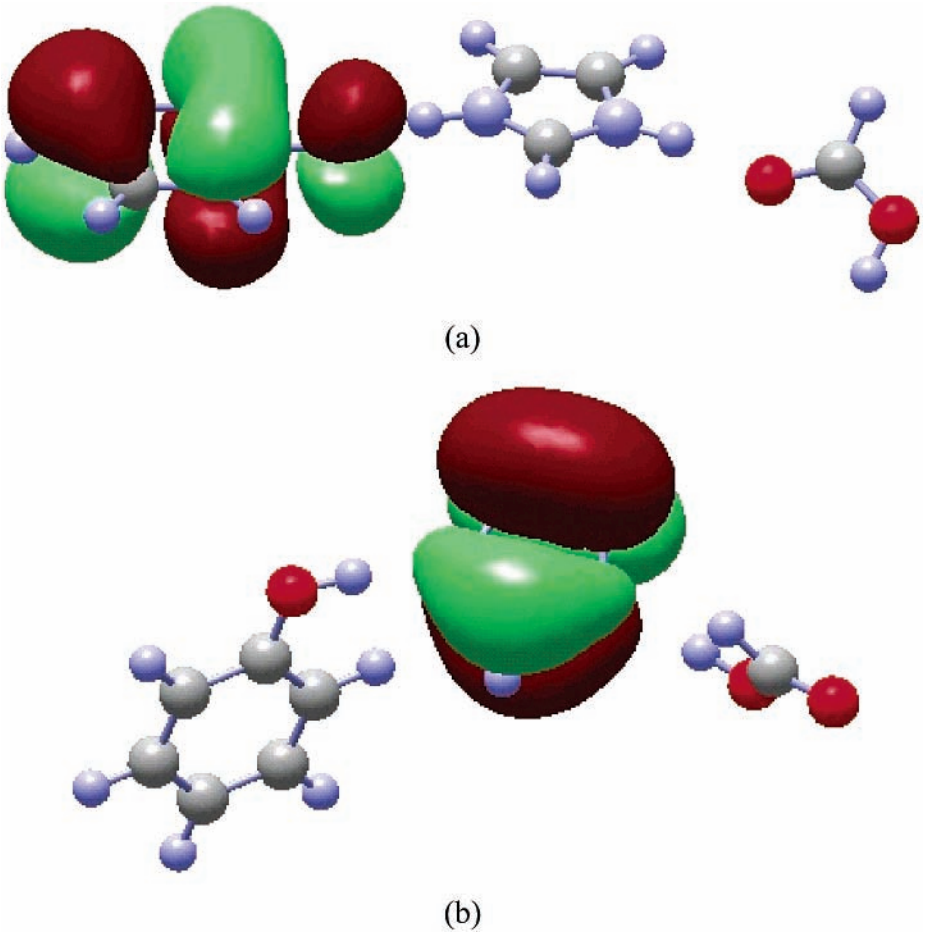

Figure 9. SOMO of the (a) phenoxyl radical cation−imidazole−formic acid complex and (b) phenoxyl radical cation−imidazole−formate complex calculated at the RMP2/6-311++g** level.

TABLE 6: The Spin Densities (from RMP2/6-311++g population) at the Phenolic Oxygens in Phenol Radical, Phenol Radical Cation, and All the Phenoxyl−Amine Complexes (both N-protonated and O-protonated) (a.u.)**

amines	phenoxyl radical complexes (the proton is on N)	phenoxyl radical cation complexes (the proton is on O)
phenoxyl radical	0.620	
phenol radical cation		0.058
NH_3	0.128	
CH_3NH_2	0.135	
imidazole	0.147	
imidazole + formate	0.220	0.000
imidazole + formic acid	0.157	
NH_2F		0.073
NF_3		0.061
NH_2CCH		0.076
NH_2CCCH_3	0.126	0.082
NH_2CCNO_2		0.065
NH_2CCF	0.116	0.076
NH_2CCOH	0.123	0.079
NH_2CCCl	0.118	0.076
$NH_2C_6H_4F$	0.136	

oxidation product is a complex between phenoxyl radical and ammonium. The shift of the adiabatic phenol oxidation potential by ammonia in the gas phase is as large as about 1 eV.

(3) Depending on the basicity of the amine, the effects of hydrogen bonding to different amines on the phenol oxidation are different. For those amines that have a proton affinity larger than ca. 204 kcal/mol, the oxidation of the pheno−amine complexes causes a proton transfer and the proton-transferred structure is the only minimum on the potential surface after oxidation. When the proton affinity of the amine is located in the range of ca. 190−197 kcal/mol, both the proton-transferred and nonproton-transferred structures are found to be minima for the oxidized complex. When the proton affinity of the amine is smaller than ca. 189 kcal/mol, no proton transfer occurs in the oxidation and the nonproton-transferred structure is the only minimum.

(4) Hydrogen bonding to amines lowers the oxidation potential of phenol. This is because the phenoxyl radical cation has a smaller proton affinity than the phenol anion, so that amine interaction with the phenoxyl radical cation is energetically more favorable than that with phenol. The shift of the adiabatic oxidation potential is roughly in linear correlation with the proton affinity of the amine. For substituted aminoacetylenes, the shift of the adiabatic oxidation potential is also in linear correlation with the Hammett σ_p substituent constants.

(5) The phenol−imidazole−formate complex is not a reasonable model for the Tyr_z oxidation in PSII, mostly because such a complex has a too low oxidation potential compared to that found for free phenol. Also, because of the strong electron donating effects of formate, in addition to phenol the imidazole moiety in the complex can also be oxidized. By contrast, the phenol−imidazole−formic acid complex is found to be a good model for PSII Tyr_z oxidation. Therefore, the Glu189 residue in PSII is probably protonated under the physiological condition.

Acknowledgment. We are grateful to the NSFC for the financial support.

References and Notes

(1) (a) Stubbe, J. A. *Annu. Rev. Biochem.* **1989**, *58*, 257. (b) Stubbe, J. A.; van der Donk, W. A. *Chem. Rev.* **1998**, *98*, 705.

(2) (a) Nugent, J. H. A.; Rich, A. M.; Evans, M. C. W. *Biochim. Biophys. Acta* **2001**, *1503*, 138. (b) Rappaport, F.; Lavergne, J. *Biochim. Biophys. Acta* **2001**, *1503*, 246.

(3) (a) MacMillan, F.; Kannt, A.; Behr, J.; Prisner, T.; Michel, H. *Biochemistry* **1999**, *38*, 9179. (b) Proshlyakov, D. A.; Pressler, M. A.; DeMaso, C.; Leykam, J. F.; DeWitt, D. L.; Babcock, G. T. *Science* **2000**, *290*, 1588.

(4) Putnam, C. D.; Arvai, A. S.; Bourne, Y.; Tainer, J. A. *J. Mol. Biol.* **2000**, *296*, 295.

(5) Whittaker, M. M.; Ballou, D. P.; Whittaker, J. W. *Biochemistry* **1998**, *37*, 8426.

(6) Perlstein, G. H.; Nguyen, D. L.; Bar, H. H.; Griffin, G.; Stubbe, R. G. *J. Proc. Natl. Acad. Sci. U.S.A.* **2001**, *98*, 10067.

(7) (a) Lee, C. Y. *FEBS Lett.* **1992,** *299*, 119. (b) Bernard, M. T.; MacDonald, G. M.; Nguyen, A. P.; Debus, R. J.; Barry, B. A. *J. Biol. Chem.* **1995**, *270*, 1589. (c) Campbell, K. A.; Peloquin, J. M.; Diner, B. A.; Tang, X. S.; Chisholm, D. A.; Britt, R. D. *J. Am. Chem. Soc.* **1997**, *119*, 4787.

(8) (a) Chaudhuri, P.; Wiegrardt, K. *Prog. Inorg. Chem.* **2001**, *50*, 151. (b) Itoh, S.; Kumei, H.; Nagatomo, S.; Kitagawa, T.; Fukuzumi, S. *J. Am. Chem. Soc.* **2001**, *123*, 2165.

(9) (a) Uhlin, U.; Eklund, H. *Nature* **1994,** *370*, 533. (b) van Dam, P. J.; Willems, J.-P.; Schmidt, P. P.; Potsch, S.; Barra, A.-L.; Hagen, W. R.; Hoffman, B. M.; Andersson, K. K.; Graslund, A. *J. Am. Chem. Soc.* **1998,** *120*, 5080. (c) Warncke, K.; Perry, M. S. *Biochim. Biophys. Acta* **2001**, *1545*, 1.

(10) (a) Tommos, C.; Skalicky, J. J.; Pilloud, D. L.; Wand, A. J.; Dutton, P. L. *Biochemistry* **1999**, *38*, 9495. (b) Tommos, C.; Babcock, G. T. *Biochim. Biophys. Acta* **2000**, *1458*, 199.

(11) (a) Nordlund, P.; Ekhund, H. *J. Mol. Biol.* **1993**, *232*, 123. (b) Sjoberg, B.-M. *Structure* **1994**, *2*, 793. (c) Rova, U.; Goodtzova, K.; Ingemarson, R.; Behravan, G.; Graslund, A.; Thelander, L. *Biochemistry* **1995**, *34*, 4267. (d) Schmidt, P. P.; Rova, U.; Thelander, L.; Graslund, A. *J. Biol. Chem.* **1998**, *273*, 21463. (e) Un, S.; Atta, M.; Fontecave, M.; Rutherford, A. W. *J. Am. Chem. Soc.* **1995**, *117*, 10713. (f) Hays, A.-M. A.; Vassiliev, I. R.; Golbeck, J. H.; Debus, R. J. *Biochemistry* **1999**, *38*, 11851. (g) Haumann, M.; Mulkidjanian, A.; Junge, W. *Biochemistry* **1999**, *38*, 1258.

(12) Blomberg, M. R. A.; Siegbahn, P. E. M.; Babcock, G. T. *J. Am. Chem. Soc.* **1998**, *120*, 8812.

(13) O'Malley, P. J. *J. Am. Chem. Soc.* **1998**, *120*, 11732.

(14) Wang, Y.-N.; Eriksson, L. A. *Int. J. Quantum Chem.* **2001**, *83*, 220.

(15) (a) Sun, L. C.; Burkitt, M.; Tamm, M.; Raymond, M. K.; Abrahamsson, M.; LeGourriérec, D.; Frapart, Y.; Magnuson, A.; Kenéz, P. H.; Brandt, P.; Tran, A.; Hammarström, L.; Styring, S.; Åkermark, B. *J. Am. Chem. Soc.* **1999**, *121*, 6834. (b) Sun, L. C.; Hammarstrom, L.; Akermark, B.; Styring, S. *Chem. Soc. Rev.* **2001,** *30*, 36.

(16) Maki, T.; Araki, Y.; Ishida, Y.; Onomura, O.; Matsumura Y. *J. Am. Chem. Soc.* **2001,** *123*, 3371.

(17) (a) Chipman, D. M. *J. Phys. Chem. A* **2000**, *104*, 11816. (b) Engstrom, M.; Himo, F.; Graslund, A.; Minaev, B.; Vahtras, O.; Agren, H. *J. Phys. Chem. A* **2000**, *104*, 5149.

(18) Frisch, M. J.; Trucks, G. W.; Schlegel, H. B.; Scuseria, G. E.; Robb, A.; Cheeseman, J. R.; Zakrzewski, V. G.; Montgomery, J. A., Jr.; Stratmann, R. E.; Burant, J. C.; Dapprich, S.; Millam, J. M.; Daniels, A. D.; Kudin, K. N.; Strain, M. C.; Farkas, O.; Tomasi, J.; Barone, V.; Cossi, M.; Cammi, R.; Mennucci, B.; Pomelli, C.; Adamo, C.; Clifford, S.; Ochterski, J.; Petersson, G. A.; Ayala, P. Y.; Cui, Q.; Morokuma, K.; Malick, D. K.; Rabuck, A. D.; Raghavachari, K.; Foresman, J. B.; Cioslowski, J.; Ortiz, J. V.; Baboul, A. G.; Stefanov, B. B.; Liu, G.; Liashenko, A.; Piskorz, P.; Komaromi, I.; Gomperts, R.; Martin, R. L.; Fox, D. J.; Keith, T.; Al-Laham, M. A.; Peng, C. Y.; Nanayakkara, A.; Gonzalez, C.; Challacombe, M.; Gill, P. M. W.; Johnson, B.; Chen, W.; Wong, M. W.; Andres, J. L.; Gonzalez, C.; Head-Gordon, M.; Replogle, E. S.; Pople, J. A. *Gaussian 98*, Revision A.7; Gaussian, Inc.: Pittsburgh, PA, 1998.

(19) Byrd, E. F. C.; Sherrill, C. D.; Head-Gordon, M. *J. Phys. Chem. A* **2001**, *105*, 9736.

(20) Hobza, P.; Sponer, J.; Reschel, T. *J. Comput. Chem.* **1995**, *11*, 1315.

(21) (a) Pakinson, C. J.; Mayer, P. M.; Radom, L. *Theor. Chim. Acta* **1999**, *102*, 92. (b) Parkinson, C. J.; Mayer, P. M.; Radom, L. *J. Chem. Soc., Perkin Trans. 2* **1999**, 2305. (c) Henry, D. J.; Parkinson, C. J.; Mayer, P. M.; Radom, L. *J. Phys. Chem. A* **2001**, *105*, 6750.

(22) Boys, S. F.; Bernardi, F. *Mol. Phys.* **1970**, *19*, 553

(23) Hobza, P.; Selzle, H. L.; Schlag, E. W. *J. Chem. Phys.* **1991**, *95*, 391.

(24) Sodupe, M.; Oliva, A.; Bertran, J. *J. Phys. Chem. A* **1997**, *101*, 9142.

(25) Sobolewski, A. L.; Domcke, W. *J. Phys. Chem. A* **2001**, *105*, 9275.

(26) Yi, M.; Scheiner, S. *Chem. Phys. Lett.* **1996**, *262*, 567.

(27) (a) Steadman, J.; Syage, J. A. *J. Am. Chem. Soc.* **1991**, *113*, 6786. (b) Syage, J. A.; Steadman, J. *J. Phys. Chem.* **1992**, *96*, 9606. (c) Mikami, N.; Okabe, A.; Suzuki, I. *J. Phys. Chem.* **1988**, *92*, 1858. (d) Mikami, N.; Sato, S.; Ishigaki, M. *Chem. Phys. Lett.* **1993**, *202*, 431. (e) Mikami, N. *Bull. Chem. Soc. Jpn.* **1995**, *68*, 683. (f) Kleinermanns, K.; Gerhards, M.; Schmitt, M. *Ber. Bunsen-Ges. Phys. Chem.* **1997**, *101*, 1785. (g) Pino, G.; Gregoire, G.; Dedonder-Lardeux, C.; Jouvet, C.; Martrenchard, S.; Solgadi, D. *Phys. Chem. Chem. Phys.* **2000**, *2*, 893

(28) (a) Abkowicz-Bienko, A. J.; Latajka, Z. *J. Phys. Chem. A* **2000**, *104*, 1004. (b) Fang Y.; Liu, L.; Guo, Q.-X. *Chem. Res. Chin. Univ.*, in press.

(29) Debus, D. J.; Campell, K. A.; Pham, D. P.; Hays, A.-M. A.; Britt, R. D. *Biochemistry* **2000**, *39*, 6275.

(30) Debus, R. J. *Biochim. Biophys. Acta* **2001**, *1503*, 164.

(31) Kim, H.-T.; Green, R. J.; Qian, J.; Anderson, S. L. *J. Chem. Phys.* **2000,** *112*, 5717.

(32) Hansch, C.; Leo, A.; Taft, R. W. *Chem. Rev.* **1991**, *91*, 165.

(33) Jiang, X.-K. *Acc. Chem. Res.* **1997**, *30*, 283.